Journal of Applied Electrochemistry (2006) 36:1083–1089
DOI 10.1007/s10800-006-9170-7

Thermal runaway of valve-regulated lead-acid batteries

JUNMEI HU, YONGLANG GUO* and XUECHOU ZHOU
College of Chemistry and Chemical Engineering, Fuzhou University, Fuzhou, 350002, PR China
*(*author for correspondence, e-mail: yguo@fzu.edu.cn)*

Received 8 October 2005; accepted in revised form 25 May 2006

Key words: oxygen recombination, saturation, thermal runaway, valve-regulated lead-acid batteries

Abstract

Valve-regulated lead-acid (VRLA) batteries that have aged on a float charge at constant voltage occasionally suffer from thermal runaway. Operating conditions for a VRLA battery have been simulated by changing the electrolyte saturation level in the separator and the ambient temperature. The charge current, battery temperature and cell overpressure were measured during current-limited constant-voltage charging. The experiments show that applied voltage, saturation level and ambient temperature are significant variables in the oxygen cycle. However, the saturation level of the electrolyte in the separator pore volume is critical. When it is lower than 80%, thermal runaway occurs readily. Significant corrosion of the positive grid and poor conductivity between the grid and the active mass (AM) is also found in aged VRLA batteries, and many inactive $PbSO_4$ crystals appear on the negative plates. As a result, both positive and negative plates have a very high resistance, which can accelerate thermal runaway.

1. Introduction

The VRLA battery is designed to operate on the concept of the ''internal oxygen cycle'', or ''oxygen recombination'' [1–10]. The electrolyte, which is starved, is immobilized by adding a gelling agent or using an absorptive glass mat (AGM) separator. At the end of charge or during overcharge, the oxygen evolving from the positive plate transfers through the gas space and/or the pores of AGM or through cracks of the gelled electrolyte to the surface of the negative plate, where it is reduced to water. The oxygen cycle causes the potential of the negative electrodes to shift in the positive direction and thereby reduces the rate of hydrogen evolution to a much lower level. Accordingly, the battery needs no maintenance [11–13]. However, a small amount of hydrogen evolution is still unavoidable, which leads to some water loss. Dry-out of electrolyte accelerates oxygen transport. Reduction of oxygen on the negative plate generates a great deal of heat. Thermal runaway may occur near the end of the battery life [14–16].

Thermal runaway is considered one of the most serious failure modes, although its incidence is small [17–18]. It depends on the difference between the rates of heat generation and its dissipation. During charging, the electrical energy introduced to cell is converted into chemical energy. Lead sulphate is converted into lead dioxide on the positive and lead on the negative plates. Subsequently the chemical energy is changed into heat energy through oxygen recombination on the negative plates. Heat effects derive from two sources. One is from the reversible heat effect of the cell reactions. The other is from Joule heating caused by the current [1, 11]. The internal oxygen cycle represents a special form of Joule heating. A temperature difference is created between the battery and the surrounding medium. Consequently, some of the heat dissipates into the surroundings. Berndt [19] suggested that heat generation has an exponential relationship with temperature, but heat dissipation has a linear relationship. When heat exchange is ineffective, the current and temperature of the battery rise quickly, resulting in thermal runaway.

Thermal runaway is usually considered to be the result of positive feedback of current and temperature when a battery is in float charge at constant voltage. There have been many published studies discussing this issue from different perspectives [20–22]. However, the mechanism and associated parameters of the processes resulting in thermal runaway are still controversial issues. The aim of this work is to probe the mechanism and influential factors of the thermal runaway processes in AGM VRLA batteries and to reduce its incidence.

2. Experimental

The battery tested was a commercial 12 V, 12 Ah VRLA electric bicycle battery with 7 positive and 8 negative plates. Its C_2 capacity was 10 Ah. A current-limited

constant voltage (CCCV) charge algorithm was applied. The charging current was 4 A until the battery reached 15.6 V (2.6 V per cell). The total charging time was about 14 h. A constant voltage of 2.6 V/cell, higher than the typical 2.4–2.5 V/cell, was used to accelerate thermal runaway.

To observe the effect of temperature on thermal runaway, charge–discharge cycles of the battery were conducted at different ambient temperatures. A temperature sensor was attached to the outside of the container to measure the battery temperature. At the same time, a pressure sensor (MP × 100D) was used to measure the overpressure inside one of the cells. The initial separator saturation was 100%. When the battery was overcharged the evolved gas was vented from cells. The resulting degree of saturation was a function of the amount of water loss and the initial electrolyte amount. In order to accelerate thermal runaway we obtained different saturations by overcharging at a constant current of 1.5 A. An Arbin Instruments BT2000 device carried out the charging–discharging of the batteries. All the data were recorded by a HP 34970A Data Acquisition/Switch Unit connected to a PC.

3. Results and discussion

In practical applications not all floated cells suffer from thermal runaway, except under extreme conditions. Experiments have shown that applied voltage is the main factor responsible for thermal runaway [21]. However, there are also other parameters which cause thermal runaway.

3.1. *Effects of separator saturation*

Figure 1 shows the evolution of the charge current during IU charging at different saturations. The experiments were carried out at a 25 °C ambient temperature. The battery was charged at a constant current (CC) for 3 h, followed by a constant voltage (CV) charge. It was obvious that the total charge current accepted by the battery went into charge, oxygen evolution and grid corrosion. Just after the transition from CC to CV charging, the charge current dropped quickly, and then maintained a low value at high saturations. With the decrease in saturation, great changes took place in the tail current. In the major course of CV, the lower the saturation, the higher was the sustained charge current. Even at 80% saturation, the charge current became increasingly high and ascended to 3.3 A at the end of charging. It was clear that after CC charging the CV charging regime caused the falling current. To compensate for the limited charge voltage, the current had to decrease and then be kept at a low value. At different saturations, the higher finishing charge current at lower saturation was caused by oxygen cycling. When saturation was low, there was more gas space in the AGM separator for the oxygen generated from the positive plates to transport to the negative ones, where the oxygen recombination occurred. Oxygen reduction shifted the potential of the negative electrode to a less negative value. Since the applied voltage was unchanged, the potential of the positive electrode shifted more positively, which in turn led to the generation of more oxygen on the positive plates. So the charge current became increasingly high. In fact, the increased current at CV was mainly used for oxygen evolution on the positive plates and for the reduction of $PbSO_4$ produced in the oxidation of Pb by oxygen on the negative plates. Because the charge efficiency never reached 100% during overcharging, the higher the overcharge current, the more $PbSO_4$ accumulated on the negative plate. Therefore, the potential shift of the positive and negative plates resulted in discharge of the negative plates. In this case the negative plate could not reach a full state-of-charge. When the battery was often undercharged the negative plates would suffer from serious irreversible sulphation, which led to PCL-3 failure [23].

Figure 2 shows the evolution of the battery temperature at different saturations. The different starting temperatures were due to different rest times after discharging. This indicates that the battery temperature

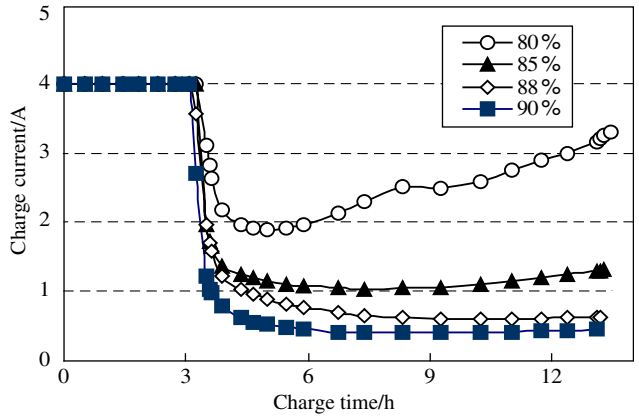

Fig. 1. Evolution of the charge current during IU charging at different saturations. Ambient temperature: 25 °C.

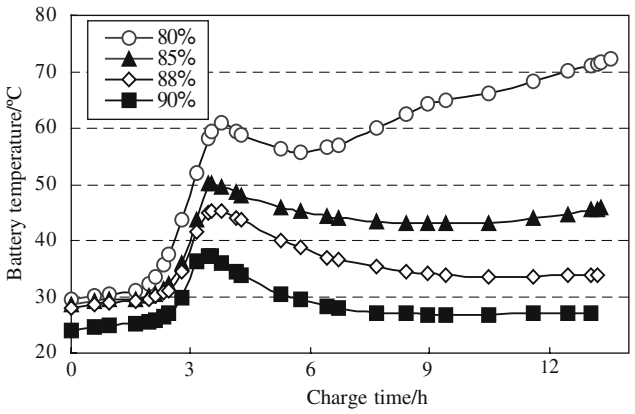

Fig. 2. Evolution of the battery temperature during IU charging at different saturations. Ambient temperature: 25 °C.

was closely associated with the saturation level. In the CC stage, the battery temperature remained almost unchanged within about 2 h and then rose rapidly. At the beginning of CC charge the lead sulphate was transformed into PbO_2 in the positive and Pb in the negative plates. Not much heat was generated with these reactions, so the battery temperature did not change much. With charging, the polarization of the positive plates increased. Then more oxygen was generated at the positive plate and oxygen recombination occurred, producing a large amount of heat that caused the battery temperature to rise rapidly. In this process Joule heating was neglected because the internal resistance of battery was very small (see Table 1, discussed in Section 3.4). A peak appeared about 15 min after CV, not just at the transition from CC to CV. This was because the temperature change lagged behind the falling current. In the following CV stage the charge current dropped continually and the recombination rate became slow, resulting in only a small amount of heat generation. Consequently, the battery temperature decreased gradually. However, at 80% saturation, the battery temperature rose to about 73 °C in the later charging. This temperature increase could lead to thermal runaway (discussed in Section 3.3). It can also be seen from Figure 2 that the lower the saturation, the higher was the battery temperature and the faster was the rate of oxygen recombination.

The evolution of overpressure in the cell at different saturations during IU charging is shown in Figure 3. At the beginning of the CC charging the overpressure decreased rapidly and the falling range was larger at lower saturation. On the one hand the chemical reactions on both the positive and negative plates made the stress on the structure of plates relax [24], causing an increase in cell space. On the other hand the lead reduced on the negative plates reacted with the oxygen in the gas space. These two factors resulted in a rapid fall in the overpressure in this period. At a lower saturation more gas space provided the channels for oxygen transport, which accelerated oxygen recombination on the negative plates. So the lower the saturation, the smaller the overpressure in the cell became. After charging for about 1 h the overpressure reached a minimum and then rose rapidly. At this time, since the potential of the positive plate increased continually, the rate of oxygen evolution was much faster than that of oxygen recombination. Once the gas pressure exceeded the limited value, the valve would open and gas would escape. So the subsequent pressure remained almost constant.

Table 1. The resistance of cell and plates

Cell	Resistance/mOhm		
	Cell	Positive plate	Negative plate
Before thermal runaway	3.18	1.10	2.20
After thermal runaway	67.74	26.74	41.17

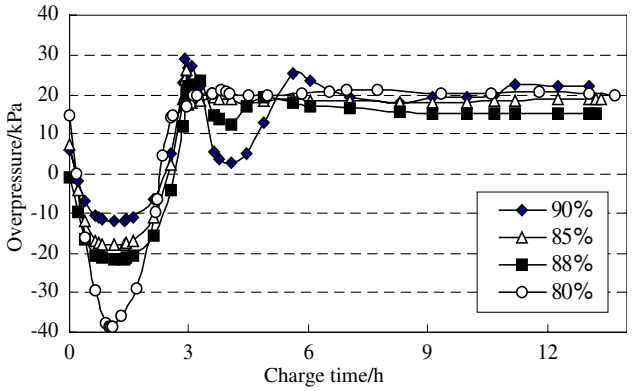

Fig. 3. Evolution of the cell overpressure during IU charging at different saturations. Ambient temperature: 25 °C.

3.2. *Effects of ambient temperature*

Figure 4 shows the evolution of the overpressure in the cell during IU charging at different ambient temperatures at 85% saturation. The overpressure falling range at 35 °C is larger than that at 25 °C. They are 55 and 29 kPa, respectively. This is because the elevated temperature accelerated oxygen transport and its recombination on the negative plates. So more oxygen in the gas space was consumed. However with increase in polarization during charging, more oxygen evolved at higher temperature, which led to a rapid rise in the overpressure.

The battery temperature evolution at different ambient temperatures is shown in Figure 5. The starting temperature is higher than the surrounding temperature, as explained in Section 3.1 (see Figure 2). In the course of CC charging the battery temperature difference between 25 and 35 °C ambient temperatures was about 10 °C. Higher ambient temperature made the battery temperature rise correspondingly. Experiments in [20] showed that an increase of 10 °C brought about a four-fold increase in the rate of oxygen evolution. But Figure 5 shows that the heat generation and its dissipation almost

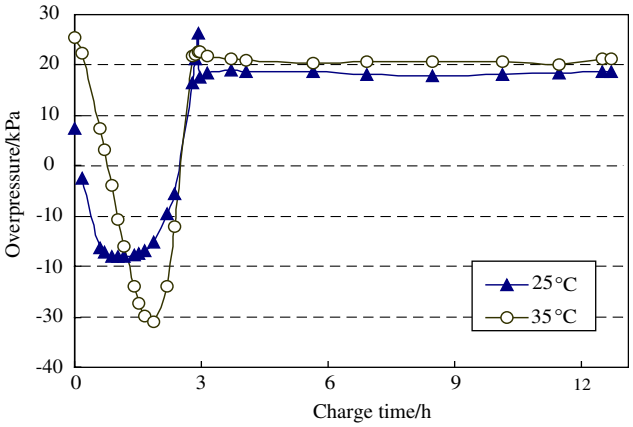

Fig. 4. Evolution of the cell overpressure during IU charging at different ambient temperatures. Saturation: 85%.

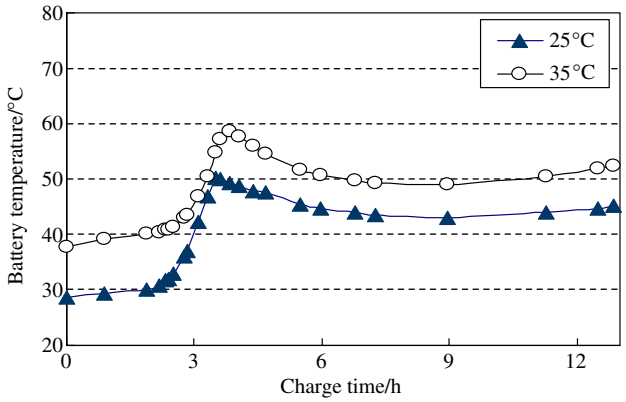

Fig. 5. Evolution of the battery temperature during IU charging at different ambient temperatures. Saturation: 85%.

reached equilibrium and the battery temperature difference between 25 and 35 °C ambient temperatures was less than 10 °C during CV charging. This is because more oxygen escapes from the valve at higher ambient temperature. This means that the oxygen recombination was not accelerated at 85% saturation because part of the oxygen escaped and the heat emanated from the battery.

3.3. *The process of thermal runaway*

Figure 6 shows the evolution of the battery temperature and the charge current during IU charging at 80% saturation. At 25 °C ambient temperature the charge current dropped and then rose slowly during CV charging. Since the saturation was relatively low, the lowest charge current was still higher than 2.1 A and at the end of charging, it was nearly six times the current at 90% saturation (see Figure 1). In the latter stages of CC charging the battery temperature rose rapidly and a peak (61 °C) appeared after several minutes of CV charging. With decrease in charge current, the battery temperature descended a little, and then rose again. At the end of CV charging the battery temperature reached 75 °C. It is obvious that both temperature and charge current are closely related to each other. Under these conditions thermal runaway could occur at any moment.

Figure 6B shows that the battery temperature rose with the increase in ambient temperature from 25 to 30 °C. When it reached 77 °C, the charge current went up exponentially over about 7 h. When the battery was charged for 7.6 h, the battery temperature reached 86 °C and the charge current was 16.5 A. At that time, thermal runaway occurred. A lot of oxygen escaped from the battery, which led to a sharp fall in the oxygen cycle current. Since the change in temperature lagged behind the heat generation or dissipation, the battery temperature rose continually and then dropped rapidly. Figure 7 shows the change in cell overpressure during IU charging at different ambient temperatures and 80% saturation. In about 3 h, the cell vent was opened and the overpressure remained almost constant at 25 °C ambient temperature. After 6 h of charging, the overpressure was falling due to the larger vent port that opened because of the high float current at 30 °C ambient temperature. At 7.6 h, the overpressure exceeded 100 kPa, which was a limiting value of the pressure sensor. At such a high temperature the battery container was distorted and thermal runaway occurred.

It is noted that the battery was out of control and appeared abnormal at 80% saturation. When the battery was severely starved there was a great deal of gas space. This promoted oxygen transport to the negative electrodes again, where the oxygen was recombined, accompanied by a large amount of heat. Since the rate of heat dissipation in the battery was slow, the battery temperature increased, thus increasing the charge current. The rate of oxygen evolution and the grid corrosion thus also increased. With the elevated ambient temperature the heat exchange between the battery and the surrounding medium became slow, and

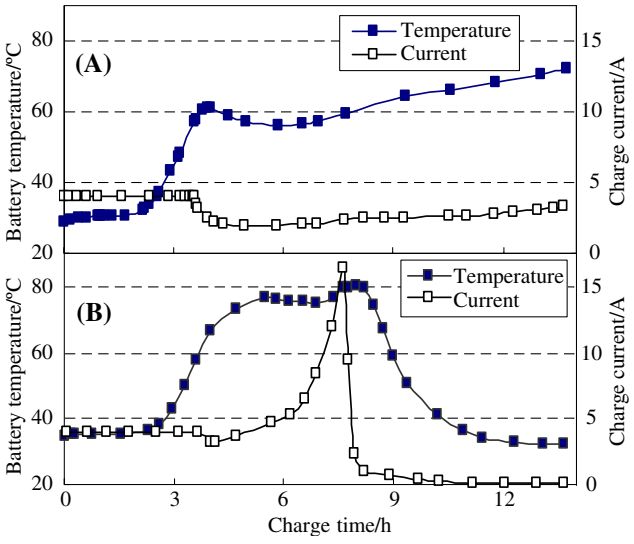

Fig. 6. Evolution of the battery temperature and the charge current during IU charging. Ambient temperature: (A) 25; (B) 30 °C. Saturation: 80%.

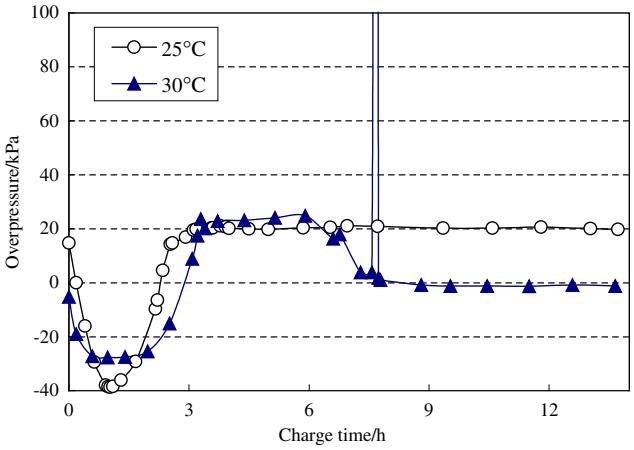

Fig. 7. Evolution of the cell overpressure during IU charging at different ambient temperatures. Saturation: 80%.

the internal oxygen cycle reactions entered into self-accelerating processes, causing the battery temperature and the charge current to increase more and more. Serious sulphation occurred on the negative plates and more electrolyte was lost [25]. After nearly 7.6 h the rate of gas evolution exceeded that of both oxygen recombination and gas release. Thermal runaway occurred. It could be expected that at lower saturation and higher ambient temperature the battery would suffer serious consequences.

3.4. *Effects of thermal runaway on active mass (AM) structure*

As mentioned in Section 3.1, the constant voltage and oxygen recombination during charging made the positive electrode potential shift positively. When thermal runaway occurred the very high temperature and violent oxygen evolution accelerated the corrosion of the positive grid, as confirmed by the scanning electron micrograph (SEM) shown in Figure 8. The corrosion layer was about 100 μm thick and the contact between grid and AM was obviously poor. This also increased the resistance of the positive plates and then the temperature of the battery.

Figure 9 shows the SEM of positive and negative active mass (PAM and NAM) of the normal plates and after thermal runaway. The NAM of the normal plate in Figure $9A_1$ has a dendritic structure. It can be seen from Figure $9A_2$ that the NAM after thermal runaway has lost its dendritic lead structure and is composed of sand-like, poorly crystallized $PbSO_4$ particles. In Figure $9B_1$, the PAM has a coralloid structure and the connection among the particles is good. For the positive plate after thermal runaway the contact between the PAM particles is very poor and many big $PbSO_4$ crystals remain in Figure $9B_2$ even though the battery temperature has risen to a very high value and the charge current has exceeded 15 A. Apparently the violent oxygen evolution caused many $PbSO_4$ crystals to lose conductivity so that they became inactive.

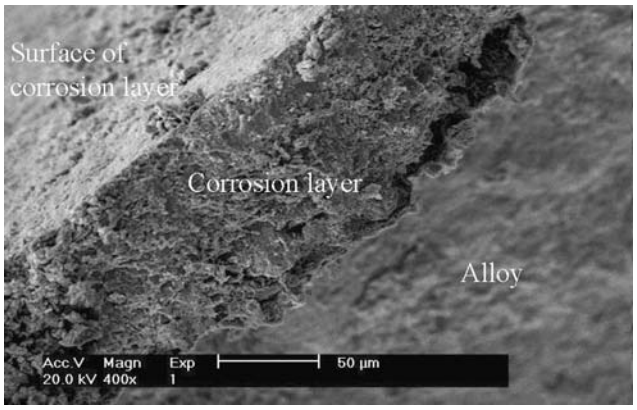

Fig. 8. Scanning electron micrograph of the cross section of the positive grid after thermal runaway.

To further confirm the results we measured the cell resistance by applying a 5 A current pulse for 1 ms to the cell and measured the response of the potentials of the positive and negative plates using a reference electrode. The resistances of the positive and negative plates including separator were thus determined and the values are shown in Table 1. Clearly the measurement includes all polarization resistance except the concentration difference. The resistance of both positive and negative plates has increased about 20 times. Evidently, the large number of inactive $PbSO_4$ crystals caused higher plates resistance.

Figure 10 shows the XRD patterns of the PAM and NAM after thermal runaway. Many $PbSO_4$ crystals remained on the positive and negative plates. While α-PbO_2 was hardly observed the β-PbO_2 was dominant along with $PbSO_4$. The violent gassing had caused loosening of the AM structure and formation of much inactive $PbSO_4$. On the negative plate the rate of oxygen recombination was so high that more $PbSO_4$ crystals were produced. Therefore, as the saturation decreased and the ambient temperature increased the oxygen cycle was accelerated and the resistance on the separator and the positive and negative plates became increasingly higher. These factors further accelerated the oxygen cycle and elevated the battery temperature. Finally thermal runaway occurred.

4. Conclusions

In AGM–VRLA batteries there are many parameters that affect thermal runaway, such as the applied voltage, saturation, ambient temperature and charge current. Most of them are important to oxygen recombination at the negative plates. The higher charge voltage increases the polarization of the positive plates, causing oxygen evolution to increase exponentially. The lower saturation levels provide more channels in the AGM separator for oxygen to transport from the positive plates to the negative plates, where oxygen is reduced. This leads to a potential shift of the negative plate in the positive direction, which makes the potential of the positive plates increase again. Therefore, the rate of oxygen recombination becomes increasingly high. As the ambient temperature is elevated, the battery temperature also rises. Then, the battery voltage on open circuit drops and polarization increases at the given charge voltage, resulting in violent oxygen evolution. Higher temperatures also accelerate oxygen transport and its recombination on the negative plates. In the extreme case, the battery temperature can exceed 80 °C. When the charge voltage, saturation and temperature reach their critical values, thermal runway occurs. Even if it does not occur, the higher temperature and oxygen cycle current at low saturation can lead to serious corrosion of the positive grid and poor conductivity between the grid and the AM. At the same time depolarization by a

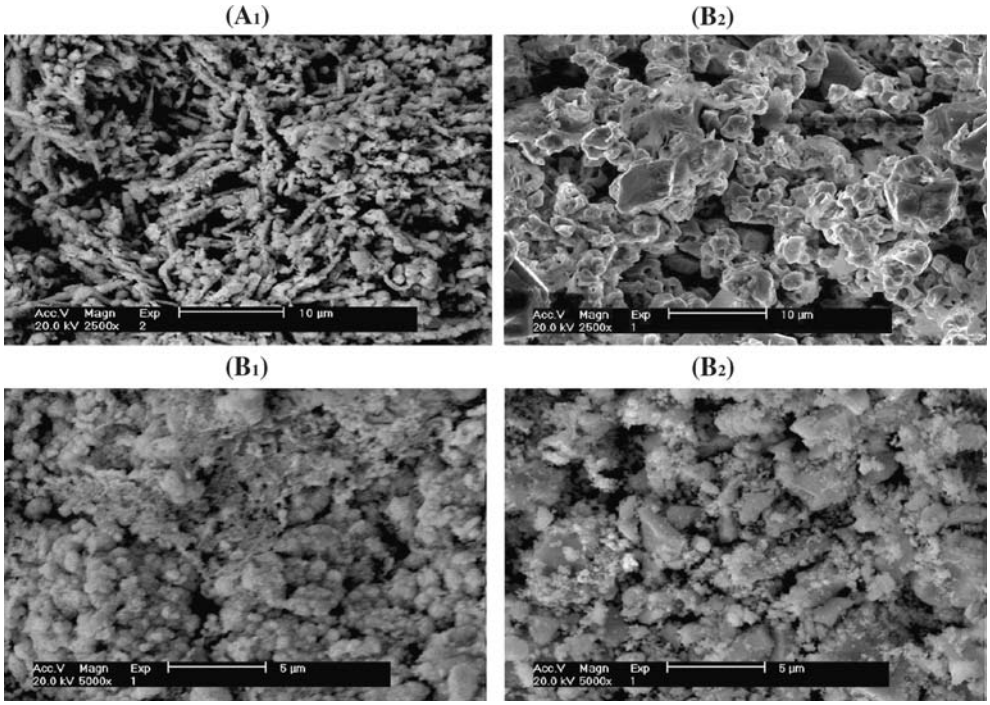

Fig. 9. Scanning electron micrographs of the active mass of (A) negative and (B) positive plates. Subscript 1 and 2 denote AM of the normal plate and after thermal runaway, respectively.

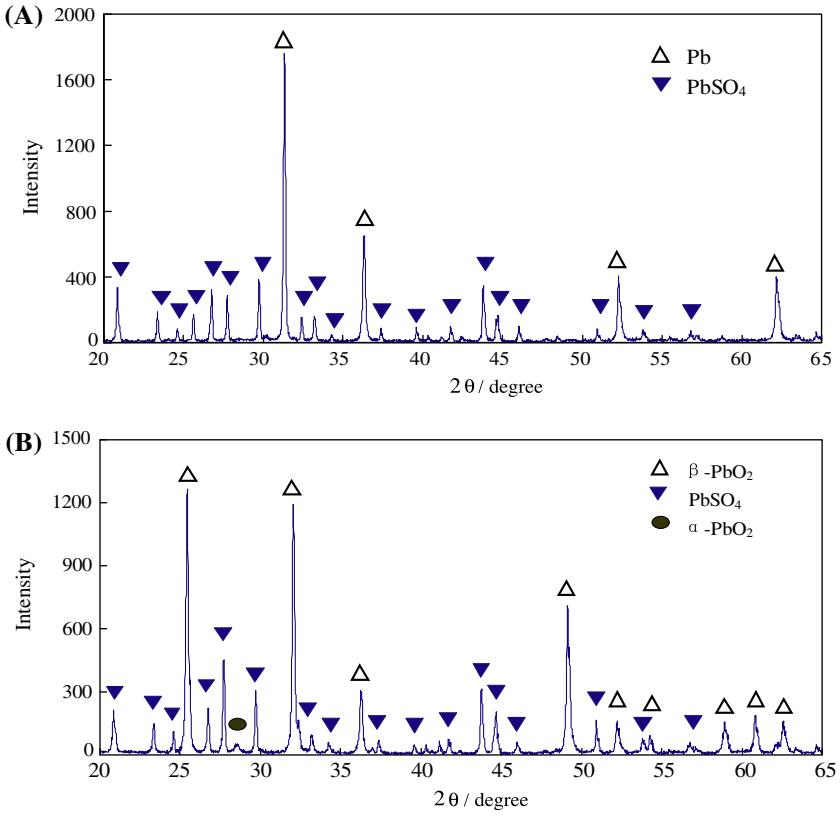

Fig. 10. XRD patterns of (A) negative and (B) positive active mass after thermal runaway.

large amount oxygen reduction causes many inactive $PbSO_4$ crystals to form on the negative plates. Thus the resistance on both the positive and negative plates increases greatly, which also accelerates thermal runaway of VRLA batteries.

Acknowledgements

The authors are grateful to NSFC (No. 20373037) in China for financial support of this work and thank Dr. Kathryn Bullock for her assistance with language.

References

1. D.A.J. Rand, P.T. Moseley, J. Garche and C.D. Parker, 'Valve-Regulated Lead-Acid Batteries' (Elsevier, Amsterdam, 2004) p. 2.
2. P.E. Pascoe and A.H. Anbuky, *Energy Conversion Manage*. **45** (2004) 1015.
3. P.T. Moseley, *J. Power Sources* **88** (2000) 71.
4. Y. Onoda, *J. Power Sources* **88** (2000) 101.
5. H. Dietz, M. Radwan, J. Garche, H. Döring and K. Wiesener, *J. Appl. Electrochem*. **21** (1991) 221.
6. J. Timmons, R. Kurian, A. Goodman and W.R. Johnson, *J. Power Sources* **136** (2004) 372.
7. R. Wagner and D.U. Sauer, *J. Power Sources* **95** (2001) 141.
8. G.J. May, *J. Power Sources* **133** (2004) 110.
9. P. Häring and H. Giess, *J. Power Sources* **95** (2001) 153.
10. Z. Li, Y. Guo, L. Wu, M. Perrin, H. Döring and J. Garche, *J. Electrochem. Soc*. **149** (2002) A934.
11. D. Berndt, *J. Power Sources* **100** (2001) 29.
12. D.A.J. Rand, P.T. Moseley, J. Garche and C.D. Parker, 'Valve-Regulated Lead-Acid Batteries' (Elsevier, Amsterdam, 2004) p. 7.
13. R.F. Nelson, Proceedings of the 4th International Lead-Acid Battery Seminar, 25-27 April (1990), San Francisco, USA, International Lead Zinc Research Organization, Inc. p. 31.
14. R.K. Jaworski and J.M. Harkins, Proceedings of the 1996 18th International Telecommunications Energy Conference, INTELEC, Oct 6–10 (1996), Boston, MA, USA p. 45.
15. S. Misra and A.J. Williamson, Proceedings of the 1998 20th International Telecommunications Energy Conference, INTELEC, Oct 4–8 (1998), San Francisco, CA, USA p. 536.
16. B. Culpin and P.L. Wainwright, *IEE Conference Publication* **484** (2001) 361.
17. W.T. Rutledge and R.J. Bowers, Proceedings of the 16th International Telecommunications Energy Conference, Vancouver, BC, Can, Oct 30–Nov 3 (1994), p. 168.
18. D. Berndt, *Maintenance-Free Batteries* (Research Studies Press, Taunton, Somerset, UK, 1993), pp. 32–157.
19. D. Berndt, *Maintenance-Free Batteries* (Wiley, New York, 1993), p. 306.
20. D. Pavlov, *J. Power Sources* **64** (1997) 131.
21. B Culpin, *J. Power Sources* **133** (2004) 79.
22. E. Boisvert, Proceedings of the 23rd International Telecommunications Energy Conference, Oct 14–18 (2001), Edinburgh, p. 126.
23. P.T. Moseley, *J. Power Sources* **95** (2001) 218.
24. M. Perrin, H. Döring, K. Ihmels, A. Weiss, E. Vogel and R. Wagner, *J. Power Sources* **95** (2001) 85.
25. K.R. Bullock, *J. Power Sources* **116** (2003) 8.